Materials Physics and Mechanics 42 (2019) 256-264 Received: October 06, 2018

BOUNDARY ELEMENT TIME-HARMONIC ANALYSIS OF 3D LINEAR PIEZOELECTRIC SOLIDS

L.A. Igumnov, I.P. Markov*, A.V. Boev

Research Institute for Mechanics, National Research Lobachevsky State University of Nizhny Novgorod, 23, bldg. 6, Gagarin Ave, Nizhny Novgorod, 603950, Russia

*e-mail: markov@mech.unn.ru

Abstract. In this work, a boundary element method (BEM) is applied for time-harmonic analysis of three-dimensional linear piezoelectric solids. Coupled frequency domain boundary value problems of the linear theory of piezoelectricity are considered assuming zero initial conditions, in the absence of the body forces and free electric charges. The elastic and electric variables are combined into the extended vectors and tensors. Proposed boundary element approach employs regularized weakly singular frequency domain boundary integral equations (BIEs) for the extended displacements. A standard collocation procedure for the mixed boundary elements is used. Integral expressions of the three-dimensional frequency domain dynamic piezoelectric fundamental solutions are employed. Results of the boundary-element analysis of a test problem are provided to validate the proposed BEM formulation.
Keywords: piezoelectricity, boundary element method, time-harmonic analysis, fundamental solutions

1. Introduction

Piezoelectric materials show two kinds of coupling effects and are extensively used to convert energy between two different forms: electric and mechanic. The direct effect consists in the ability to accumulate electric charge as a response to applied mechanical loads; the converse effect is characterized by the ability to produce mechanical deformation when electric loads are applied. Piezoelectric materials proved to be indispensable and very effective in many engineering applications such as vibration-based energy harvesters [1–3], microelectromechanical systems devices [4,5], active damping in structural vibrations, acoustic noise suppression, etc. To utilize the potential of piezoelectric structures subjected to transient dynamic or time-harmonic loadings to full extent it is essential to properly model their coupled behavior with reliable numerical method.

Various numerical techniques, such as Finite Difference Method (FDM) or Finite Element Method (FEM), can be employed to study dynamic behavior of complex piezoelectric structures. Among them is Boundary Element Method, a well-known boundary integral equations based method. Compared to the domain-based numerical methods like FDM and FEM, BEM has the distinct advantage of unknown field variables being located only on the boundary of the domain under consideration. This feature leads to the lack of necessity to mesh the interior of the domain, which results in the smaller number of unknowns in the discrete model.

The development of conventional direct boundary element procedure for transient dynamic and time-harmonic problems in linear piezoelectric solids as usual relies on reduction of the boundary value problems to a corresponding system of boundary integral

http://dx.doi.org/10.18720/MPM.4222019_12

equations with utilization of the reciprocal theorem and fundamental solutions. It is known, that the dynamic fundamental solutions and the corresponding stress fields for generally anisotropic piezoelectric materials are not available in the closed-form expressions. Various approaches for numerical and semi-analytical treatment of the static anisotropic elastic and piezoelectric fundamental solutions were proposed (e.g. [6–13]). Review of the available scientific literature reveals only a few BEM implementations concerning time-harmonic analysis for piezoelectric solids [14–18] including those based on Dual Reciprocity approach, which utilizes only the static fundamental solution.

In this paper, a formulation of the frequency domain direct boundary element approach is present and applied for the time-harmonic analysis of three-dimensional (3D) homogeneous anisotropic and linear piezoelectric solids. The boundary integral equations are regularized employing the static part of the fundamental solution. The frequency domain displacement fundamental solutions for linear piezoelectric material are expressed in an integral form. Mixed boundary elements and standard collocation procedure are used for the spatial discretization. The versatility and reliability of the proposed formulation is demonstrated by numerical examples for piezoelectric solid under complex electro-mechanical loading. The obtained boundary element results are compared with those obtained by a finite element method.

2. Problem statement

Consider a three-dimensional homogeneous finite anisotropic and piezoelectric solid $\Omega \in R^3$ with smooth boundary $\Gamma = \partial\Omega$. Piezoelectric linear constitutive equations are given as follows [19,20]:

$$\sigma_{ij} = C^E_{ijkl} s_{kl} - e_{ijk} E_k, \quad i, j, k, l = \overline{1,3}, \tag{1}$$

$$D_i = e_{ikl} s_{kl} + \varepsilon_{ik} E_k, \tag{2}$$

where σ_{ij} is the stress tensor, D_i are the electric displacements, s_{kl} is the strain tensor and E_k is the electric field. The tensors C^E_{ijkl}, e_{ijk} and ε_{ik} denote, respectively, the elastic stiffness constants, the piezoelectric coupling coefficients and the dielectric properties.

For the generally anisotropic piezoelectric material, the following symmetry conditions are satisfied:

$$C^E_{ijkl} = C^E_{klij} = C^E_{jikl} = C^E_{ijlk}, \tag{3}$$

$$e_{ijk} = e_{ikj}, \tag{4}$$

$$\varepsilon_{ij} = \varepsilon_{ji}. \tag{5}$$

Applying the quasi-electrostatic assumption, the strain – displacement and the electric field – electric potential relationships are written as

$$s_{ij} = \frac{1}{2}(u_{i,j} + u_{j,i}), \tag{6}$$

$$E_i = -\phi_{,i}, \tag{7}$$

where u_i are the elastic displacements and φ is the electric potential.

In the absence of applied volume forces and free electrical charges the equilibrium equations and the electrical balance equations (the electrostatic equations) in the time domain are given as follows

$$\sigma_{ij,j} = \rho \ddot{u}_i, \tag{8}$$

$$D_{i,i} = 0, \tag{9}$$

where ρ is the mass density.

It is practical to combine the elastic and electric variables into the extended vectors and matrices using the extended notation [6] as follows

$$U_k = \begin{cases} u_k, k = \overline{1,3}, \\ \phi, \ k = 4, \end{cases} \tag{10}$$

$$S_{kl} = \begin{cases} s_{kl}, \ \ k,l = \overline{1,3}, \\ -E_l, k = 4, l = \overline{1,3}, \end{cases} \tag{11}$$

$$\Sigma_{ij} = \begin{cases} \sigma_{ij}, i, j = \overline{1,3}, \\ D_i, i = \overline{1,3}, \ j = 4, \end{cases} \tag{12}$$

$$C_{ijkl} = \begin{cases} C^E_{ijkl}, i, j, k, l = \overline{1,3}, \\ e_{lij}, \ \ i,l, j = \overline{1,3}, k = 4, \\ e_{ikl}, \ \ i,l,k = \overline{1,3}, j = 4, \\ -\varepsilon_{il} \ \ i,l = \overline{1,3}, k, j = 4. \end{cases} \tag{13}$$

Considering the symmetry conditions (3) – (5) we can write the following relationship for the extended piezoelectricity matrix C_{ijkl}:

$$C_{ijkl} = C_{lkji}. \tag{14}$$

Taking into account the extended notation (10) – (13) we rewrite the time-domain equations of motion of a linear piezoelectric solid in a simplified form in terms of the extended displacements:

$$C_{ijkl} U_{k,il} = \rho \delta^*_{jk} \ddot{U}_k, \ \ i,l = \overline{1,3}, \quad j,k = \overline{1,4}, \tag{15}$$

$$\delta^*_{jk} = \begin{cases} \delta_{jk}, \ j,k = \overline{1,3}, \\ 0, \quad \text{otherwise}. \end{cases} \tag{16}$$

We consider vanishing initial conditions and the following boundary conditions:

$$U_i(\mathbf{x},t) = \dot{U}_i(\mathbf{x},t) = 0, \ t \le 0, \tag{17}$$

$$U_i(\mathbf{x},t) = U^*_i(\mathbf{x},t), \ \ \mathbf{x} \in \Gamma_U, \tag{18}$$

$$T_i(\mathbf{x},t) = T^*_i(\mathbf{x},t), \ \ \mathbf{x} \in \Gamma_T, \tag{19}$$

where Γ_U is the part of Γ on which the extended displacements $U_i(\mathbf{x},t)$ have the prescribed values U^*_i and Γ_T is the part of Γ on which the extended tractions T_k:

$$T_k = \begin{cases} t_k = \sigma_{ik} n_k, \ k = \overline{1,3}, \\ D_n = D_i n_i, k = 4, \end{cases} \tag{20}$$

have the prescribed values T^*_i with n_i being the outward unit normal vector.

For the prescribed frequency ω and zero initial conditions (17), we rewrite the governing equations (15) and boundary conditions (18) – (19) in the frequency domain:

$$C_{ijkl} \bar{U}_{k,il} + \rho \omega^2 \delta^*_{jk} \bar{U}_k = 0, \ \ i,l = \overline{1,3}, \quad j,k = \overline{1,4}, \tag{21}$$

$$\bar{U}_i(\mathbf{x},\omega) = \bar{U}^*_i(\mathbf{x},\omega), \ \ \mathbf{x} \in \Gamma_U, \tag{22}$$

$$\bar{T}_i(\mathbf{x},\omega) = \bar{T}^*_i(\mathbf{x},\omega), \ \ \mathbf{x} \in \Gamma_T, \tag{23}$$

where overbar denotes a variable in the frequency domain.

3. BEM formulation

In the present work, we use the frequency domain direct BEM approach to solve the linear boundary-value problem defined in equations (21) – (23). To solve the prescribed boundary-value problem first it is needed to be reformulated as boundary integral equations. For the extended displacement in the frequency domain, the following system of non-strongly

singular BIEs can be obtained using the static singular part of the piezoelectric traction fundamental solution:

$$\int_{\Gamma}\left[\bar{U}_k(\mathbf{y},\omega)\bar{h}_{jk}(\mathbf{y},\mathbf{x},\omega)-\bar{U}_k(\mathbf{x},\omega)h^S_{jk}(\mathbf{y},\mathbf{x},\omega)\right]\mathrm{d}\Gamma(\mathbf{y})-\int_{\Gamma}\bar{T}_k(\mathbf{y},\omega)\bar{g}_{jk}(\mathbf{y},\mathbf{x},\omega)\mathrm{d}\Gamma(\mathbf{y})=0, \tag{24}$$

where $\bar{g}_{jk}$, $\bar{h}_{jk}$ and h^S_{jk} are the frequency domain dynamic piezoelectric extended displacement and traction fundamental solutions and the static part of traction fundamental solution, respectively; $\mathbf{x}\in\Gamma$ is the source point and $\mathbf{y}$ is the field point. All integrals in the regularized boundary integral equations (24) have the $O(1/r)$ singularity.

For numerical solving the BIEs (24), we follow the standard boundary element procedure and start with the discretization of the boundary Γ. Geometry of the boundary is approximated with the quadrangular boundary elements with quadratic shape functions. To describe the behavior of the extended displacements and tractions on the boundary elements we implement the mixed representation approach: for the displacements, linear interpolation functions are adopted and tractions are approximated by constant functions. After collocation procedure a system of complex-valued linear algebraic equations is obtained for the prescribed frequency ω:

$$\left[\bar{\mathbf{A}}(\omega)\right]\left\{\bar{\mathbf{p}}(\omega)\right\}=\left\{\bar{\mathbf{f}}(\omega)\right\}, \tag{25}$$

where $\left[\bar{\mathbf{A}}(\omega)\right]$ is the rearranged system matrix according to the boundary conditions, $\left\{\bar{\mathbf{f}}(\omega)\right\}$ and $\left\{\bar{\mathbf{p}}(\omega)\right\}$ are the vectors, containing the known and unknown boundary data.

4. Frequency domain piezoelectric fundamental solutions

For homogeneous generally anisotropic linear piezoelectric solids, dynamic fundamental solutions are not available in an explicit form. Representations of the fundamental solutions in the frequency domain can be separated into singular (static, denoted with superscript "*S*") and regular (dynamic, denoted with superscript "*D*") parts as

$$\bar{g}_{ij}(\mathbf{y},\mathbf{x},\omega)=\bar{g}_{ij}(\mathbf{r},\omega)=g^S_{ij}(\mathbf{r})+\bar{g}^D_{ij}(\mathbf{r},\omega), \tag{26}$$

$$\bar{h}_{ij}(\mathbf{y},\mathbf{x},\omega)=\bar{h}_{ij}(\mathbf{r},\omega)=h^S_{ij}(\mathbf{r})+\bar{h}^D_{ij}(\mathbf{r},\omega), \tag{27}$$

with $\mathbf{r}=\mathbf{y}-\mathbf{x}$, $r=|\mathbf{r}|$.

Using the approach based on the application of the Radon transform [21,22] the expressions for the dynamic and static parts of the piezoelectric displacement fundamental solutions are given as follows [11]:

$$\bar{g}^D_{jp}(\mathbf{r},\omega)=\frac{i}{8\pi^2}\int_{\substack{|\mathbf{n}|=1\\ \mathbf{n}\cdot\mathbf{r}>0}}\sum_{m=1}^{Q}\frac{k_m\bar{P}^m_{jp}(\mathbf{n})}{\rho c_m^2}e^{ik_m|\mathbf{n}\cdot\mathbf{r}|}dS(\mathbf{n}),\quad j,p=\overline{1,4}, \tag{28}$$

$$g^S_{jp}(\mathbf{r})=\frac{1}{8\pi^2 r}\int_{|\mathbf{d}|=1}\Gamma^{-1}_{jp}(\mathbf{d})dL(\mathbf{d}), \tag{29}$$

here

$$\bar{P}^m_{jp}=\begin{cases}P^m_{jp}, & j,p=\overline{1,3},\\ -\dfrac{\Gamma_{k4}P^m_{jk}}{\Gamma_{44}}, & j=\overline{1,3},\ p=4,\\ \dfrac{\Gamma_{4k}P^m_{kl}\Gamma_{l4}}{\Gamma^2_{44}}, & j=p=4,\end{cases} \tag{30}$$

$$P_{jp}^m = \frac{A_{jp}^m}{A_{ii}^m},\ \ A_{jp}^m = \mathrm{adj}\left(L_{jp} - \rho c_m^2 \delta_{jp}\right),\ \ L_{jp}(\mathbf{n}) = \Gamma_{jp}(\mathbf{n}) - \frac{\Gamma_{j4}(\mathbf{n})\Gamma_{4p}(\mathbf{n})}{\Gamma_{44}(\mathbf{n})}, \tag{31}$$

$$c_m = \sqrt{\frac{\lambda_m}{\rho}},\ \ k_m = \frac{\omega}{c_m},\ \ \Gamma_{ij}(\mathbf{d}) = C_{kijl} d_k d_l,\ \ \Gamma_{ij}(\mathbf{n}) = C_{kijl} n_k n_l, \tag{32}$$

where λ_m are the Q distinct eigenvalues of L_{jp}.

The variables involved in the definition of domains of integration (see Fig. 1), i.e. a half of a unit sphere for the dynamic part and a unit circumference for the static part are defined as follows:

$$dL\left(\mathbf{d}(\varphi)\right) \in D^S = \{0 \le \varphi \le 2\pi\},\ \ dS\left(\mathbf{n}(b,\varphi)\right) \in D^D = \{0 \le b \le 1;\ 0 \le \varphi \le 2\pi\}, \tag{33}$$

$$\mathbf{n}(b,\varphi) = \sqrt{1-b^2}\,\mathbf{d} + b\mathbf{e},\ \ \mathbf{e} = \mathbf{r}/r,\ \ \mathbf{e} = \left[e_1, e_2, e_3\right], \tag{34}$$

$$\mathbf{d}(\varphi) = \frac{\left[e_2 \cos\varphi + e_1 e_3 \sin\varphi, -e_1 \cos\varphi + e_2 e_3 \sin\varphi, -\left(1-e_3^2\right)\sin\varphi\right]}{\sqrt{1-e_3^2}}. \tag{35}$$

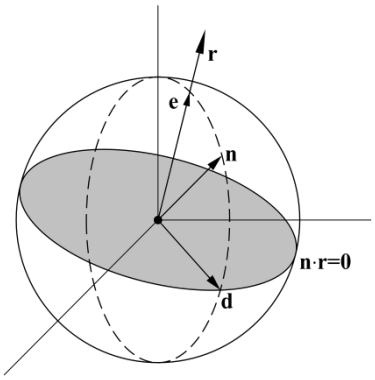

Fig. 1. Geometry of **r**, **e**, **n** and **d**

For the unit normal vector to the boundary $n_i(\mathbf{y})$ at the field point **y**, the piezoelectric traction fundamental solutions are defined by

$$\overline{h}_{jp}(\mathbf{y},\mathbf{x},\omega) = C_{ijkl}\overline{g}_{kp,l}(\mathbf{y},\mathbf{x},\omega) n_i(\mathbf{y}),\ \ j,p = \overline{1,4}. \tag{36}$$

5. Numerical example

Our test model involves rectangular piezoelectric solid as shown in Fig. 2. The solid is clamped at $x_3 = 0$ m. On the surface $x_2 = 0.2$ m the electric potential is assumed to be zero. Two cases of harmonic excitation on the surface $x_3 = 1$m is considered: traction $t_3 = -1 \cdot 10^9$ Pa and electric potential $\phi = 0$ V (case A), traction $t_3 = -1 \cdot 10^9$ Pa and electric displacements $D_n = 1\,\mathrm{C/m}^2$ (case B). Other surfaces are free of the extended tractions. For both loading cases, two frequencies are considered: $\omega_1 = 10000$ rad/s and $\omega_2 = 20000$ rad/s.

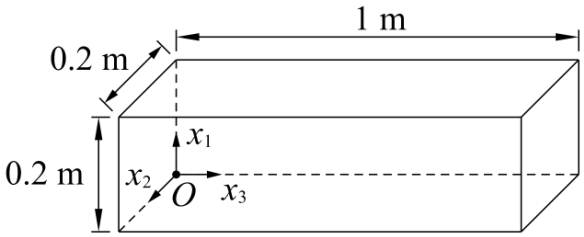

Fig. 2. A rectangular piezoelectric solid

PVDF is chosen as a piezoelectric material, which has the mass density $\rho = 1780$ kg/m^3 and the following material parameters:

$$\mathbf{C}^E = \begin{bmatrix} 238 & 3.98 & 2.19 & 0 & 0 & 0 \\ 3.98 & 23.6 & 1.92 & 0 & 0 & 0 \\ 2.19 & 1.92 & 10.6 & 0 & 0 & 0 \\ 0 & 0 & 0 & 2.15 & 0 & 0 \\ 0 & 0 & 0 & 0 & 4.4 & 0 \\ 0 & 0 & 0 & 0 & 0 & 6.43 \end{bmatrix} \text{GPa}, \tag{37}$$

$$\boldsymbol{\varepsilon} = \begin{bmatrix} 1.1068 & 0 & 0 \\ 0 & 1.0607 & 0 \\ 0 & 0 & 1.0607 \end{bmatrix} \cdot 10^{-10}\, \text{C/Vm}, \tag{38}$$

$$\mathbf{e} = \begin{bmatrix} 0 & 0 & 0 & 0 & -0.01 & 0 \\ 0 & 0 & 0 & -0.01 & 0 & 0 \\ -0.13 & -0.14 & -0.28 & 0 & 0 & 0 \end{bmatrix} \text{C/m}^2. \tag{39}$$

The solid is uniformly meshed with 1408 boundary elements in total. For loading case A, Figs. 3 – 6 and for loading case B, Figs. 7 – 10 show a comparison of the obtained BEM solutions and results of FEM analyses for the displacements u_2 and u_3, electric potential ϕ and electric displacements D_n. Results for the u_2, u_3 ϕ are calculated along the line $(0.1, 0, x_3)$ and for the D_n along the line $(0.1, 0.2, x_3)$.

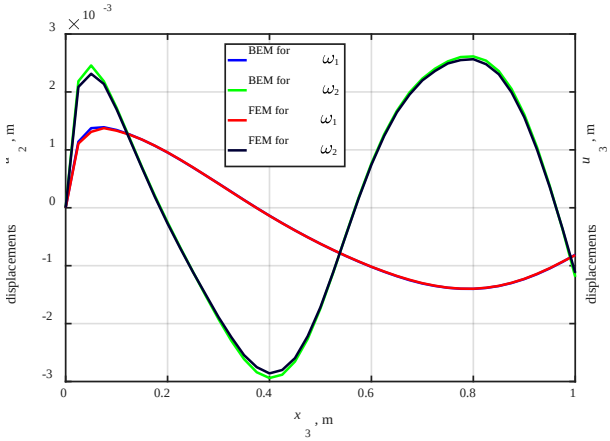

Fig. 3. Displacements $u_2(0.1, 0, x_3)$

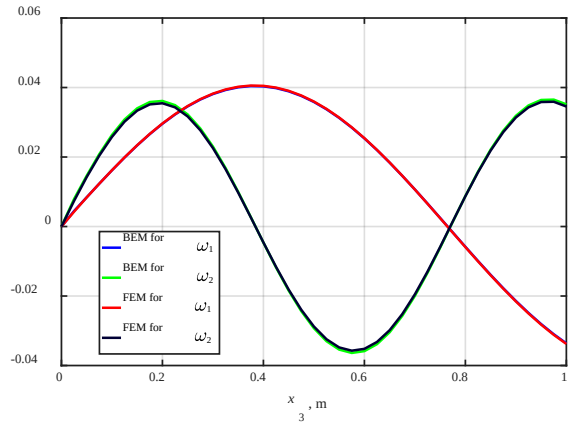

Fig. 4. Displacements $u_3(0.1, 0, x_3)$

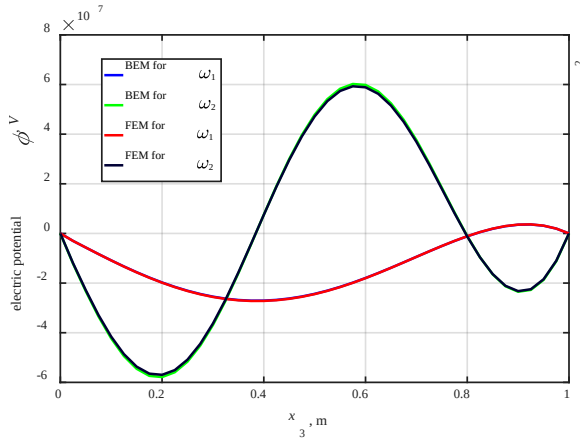

Fig. 5. Electric potential $\phi(0.1,0,x_3)$

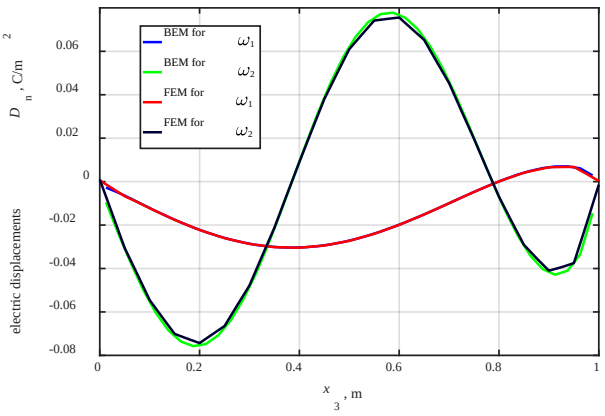

Fig. 6. Electric displacements $D_n(0.1,0.2,x_3)$

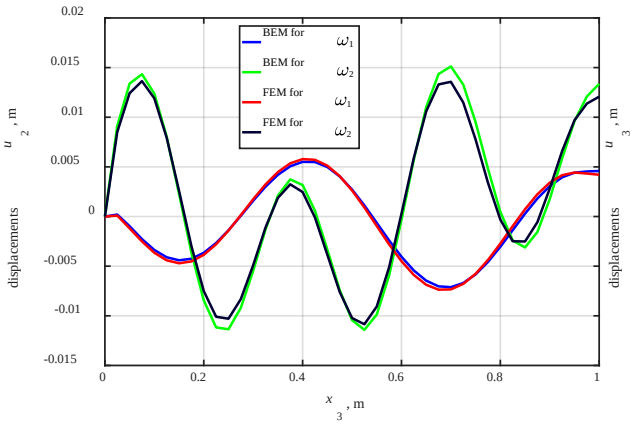

Fig. 7. Displacements $u_2(0.1,0,x_3)$

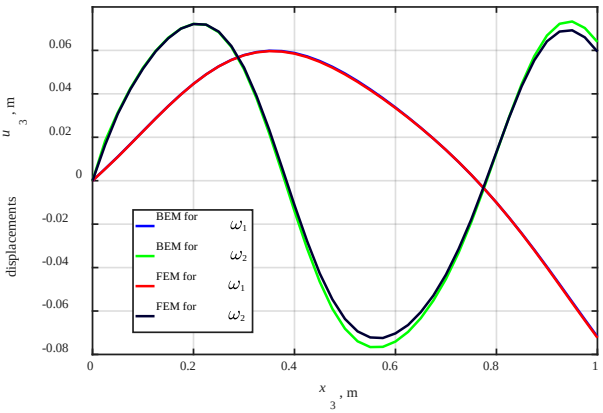

Fig. 8. Displacements $u_3(0.1,0,x_3)$

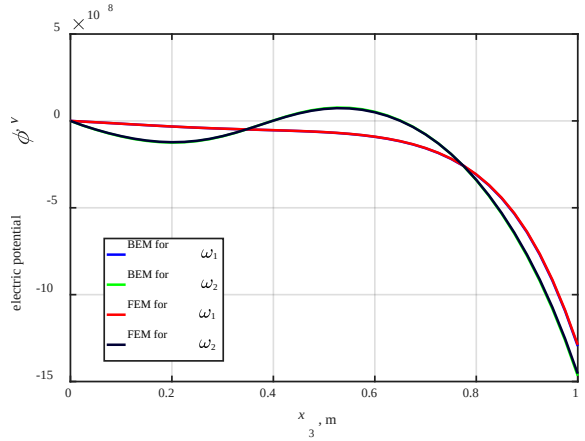

Fig. 9. Electric potential $\phi(0.1,0,x_3)$

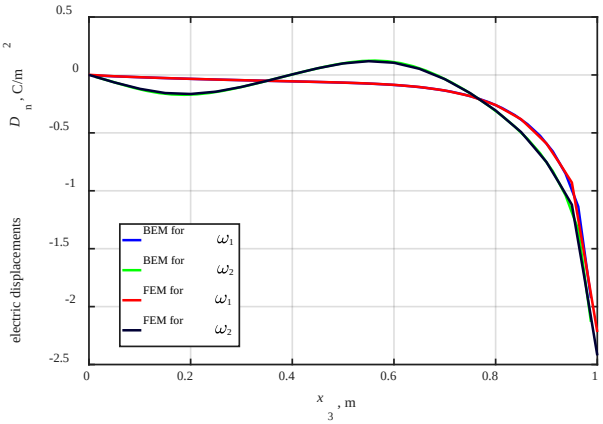

Fig. 10. Elect. displacements $D_n(0.1,0.2,x_3)$

6. Conclusions

The frequency domain boundary element formulation based on non-strongly singular displacement BIEs for homogeneous three-dimensional linear piezoelectric solids is presented. Mixed boundary elements are used for the spatial discretization. Integral expressions of the piezoelectric fundamental solutions are adopted. The versatility and reliability of the present boundary element formulation for time-harmonic piezoelectric

analysis is demonstrated by numerical examples. Obtained solutions show good agreement with the finite element results.

Acknowledgements. *The reported study was funded by Russian Foundation for Basic Research (RFBR), according to the research project No. 16-38-60097 mol_a_dk.*

References

[1] Arroyo E, Badel A, Formosa F, Wu Y, Qiu J. Comparison of electromagnetic and piezoelectric vibration energy harvesters: Model and experiments. *Sensors and Actuators A: Physical*. 2012;183: 148-156. Available from: doi.org/10.1016/j.sna.2012.04.033.

[2] Erturk A, Inman D. Piezoelectric energy harvesting. Chichester: Wiley; 2011. Available from: doi.org/10.1002/9781119991151.

[3] Siddique A, Mahmud S, Heyst B. A comprehensive review on vibration based micro power generators using electromagnetic and piezoelectric transducer mechanisms. *Energy Conversion and Management.* 2015;106: 728-747. Available from: doi.org/10.1016/j.enconman.2015.09.071.

[4] Trolier-McKinstry S, Muralt P. Thin Film Piezoelectrics for MEMS. *Journal of Electroceramics*. 2004;12(1/2): 7-17. Available from: doi.org/10.1023/b:jecr.0000033998.72845.51.

[5] Smith G, Pulskamp J, Sanchez L, Potrepka D, Proie R, Ivanov T et al. PZT-Based Piezoelectric MEMS Technology. *Journal of the American Ceramic Society*. 2012;95(6): 1777-1792. Available from: doi.org/10.1111/j.1551-2916.2012.05155.x.

[6] Barnett D, Lothe J. Dislocations and line charges in anisotropic piezoelectric insulators. *physica status solidi (b).* 1975;67(1): 105-111. Available from: doi.org/10.1002/pssb.2220670108.

[7] Ting T. The three-dimensional elastostatic Green's function for general anisotropic linear elastic solids. *The Quarterly Journal of Mechanics and Applied Mathematics*. 1997;50(3): 407-426. Available from: doi.org/10.1093/qjmam/50.3.407.

[8] Wu K. Generalization of the Stroh Formalism to 3-Dimensional Anisotropic Elasticity. *Journal of Elasticity*. 1998;51(3): 213-225. Available from: doi.org/10.1023/a:1007523219357.

[9] Nakamura G, Tanuma K. A formula for the fundamental solution of anisotropic elasticity. *The Quarterly Journal of Mechanics and Applied Mathematics*. 1997;50(2): 179-194. Available from: doi.org/10.1093/qjmam/50.2.179.

[10] Pan E, Tonon F. Three-dimensional Green’s functions in anisotropic piezoelectric solids. *International Journal of Solids and Structures*. 2000;37(6): 943-958. Available from: doi.org/10.1016/s0020-7683(99)00073-6.

[11] Wang C, Zhang C. 3-D and 2-D Dynamic Green's functions and time-domain BIEs for piezoelectric solids. *Engineering Analysis with Boundary Elements*. 2005;29(5): 454-465. Available from: doi.org/10.1016/j.enganabound.2005.01.006.

[12] Shiah Y, Tan C, Wang C. Efficient computation of the Green's function and its derivatives for three-dimensional anisotropic elasticity in BEM analysis. *Engineering Analysis with Boundary Elements*. 2012;36(12): 1746-1755. Available from: doi.org/10.1016/j.enganabound.2012.05.008.

[13] Xie L, Zhang C, Hwu C, Sladek J, Sladek V. On two accurate methods for computing 3D Green′s function and its first and second derivatives in piezoelectricity. *Engineering Analysis with Boundary Elements*. 2015;61: 183-193. Available from: doi.org/10.1016/j.enganabound.2015.07.014.

[14] Hill L, Farris T. Three-Dimensional Piezoelectric Boundary Element Method. *AIAA Journal*. 1998;36(1): 102-108. Available from: doi.org/10.2514/2.358.

[15] Kogl M, Gaul L. Dual reciprocity Boundary Element Method for three-dimensional problems of dynamic piezoelectricity. In: Brebbia CA, Power H (eds.) *WIT Transactions on Modelling and Simulation*. Southampton: WIT Press; 1999;25. p.537-548. Available from: https://www.witpress.com/elibrary/wit-transactions-on-modelling-and-simulation/25/6054 [Accessed 26th March 2019].
[16] Kogl M, Gaul L. A boundary element method for transient piezoelectric analysis. *Engineering Analysis with Boundary Elements*. 2000;24(7-8): 591-598. Available from: doi.org/10.1016/s0955-7997(00)00039-4.
[17] Denda M, Araki Y. 2-D general anisotropic and piezoelectric time-harmonic BEM for eigenvalue analysis. In: Smyth AW (ed.) *Proceedings of the 15th ASCE Engineering Mechanics Conference*. New York: Columbia University; 2002; p.77-84.
[18] Gaul L, Kogl M, Wagner M. *Boundary element methods for engineers and scientists*. Berlin: Springer; 2003.
[19] Parton VZ, Kudryavtsev BA. *Electrocmagnetoelasticity*. New York: Gordon and Breach Science Publishers; 1988.
[20] Tiersten HF. *Linear Piezoelectric Plate Vibrations*. Boston, MA: Springer US; 1969.
[21] Wang C, Achenbach J. Elastodynamic fundamental solutions for anisotropic solids. *Geophysical Journal International*. 1994;118(2): 384-392. Available from: doi.org/10.1111/j.1365-246x.1994.tb03970.x.
[22] Wang C, Achenbach J. Three-Dimensional Time-Harmonic Elastodynamic Green's Functions for Anisotropic Solids. *Proceedings of the Royal Society A: Mathematical, Physical and Engineering Sciences*. 1995;449(1937): 441-458. Available from: doi.org/10.1098/rspa.1995.0052.